Space-time dynamics of wide-gain-section lasers

P. K. Jakobsen, J. V. Moloney, A. C. Newell, and R. Indik
Department of Mathematics, University of Arizona, Tucson, Arizona 85721
(Received 10 June 1991; revised manuscript received 24 October 1991)

The space-time behavior of a wide-gain-section, single-longitudinal-mode laser is investigated. Analysis of the full Maxwell-Bloch model in one transverse spatial dimension identifies a traveling-wave solution beyond the first laser threshold, for positive detuning from resonance, which appears to be a globally attracting state of the laser. On the negative-detuning side we observe an initial bifurcation to a homogeneous plane-wave state. A second instability threshold can be identified by linearizing about the respective solutions for both positive and negative detuning. We also find that the standard approach to adiabatic elimination, whereby the polarization equation is adiabatically eliminated, can lead to a spurious high-transverse-wave-number instability in the reduced equations. The derivation of an adiabatically reduced set of equations to remove the instability on the positive-detuning side is a nontrivial matter.

PACS number(s): 42.50.−p, 42.55.Px, 42.60.Gd

INTRODUCTION

In recent years the effect of diffraction on the stability characteristics of wide-area lasers has been the focus of much effort [1–4]. We investigate the effect of diffraction on both the lasing threshold and on the stability of the lasing state for the detuned Maxwell-Bloch equations in one transverse space dimension. By performing a linear-stability analysis on the nonlasing state we find that for negative detuning the nonlasing state is unstable to the growth of a uniform amplitude perturbation. For positive detuning, on the other hand, we find that the presence of diffraction will favor growth of perturbations in bands centered on the wave numbers $\pm k_0$, where $k_0=\sqrt{\gamma_1\Delta/a}$, and where a is the diffraction, Δ is the detuning, and γ_1 is the polarization decay time. This behavior represents potential problems for the paraxial-wave approximation used to derive the model equations. For the model to be valid the parameters must be chosen such that the wave numbers $\pm k_0$ are not too large. The issue of wave-number selection at the first threshold is also important when one studies the stability of the lasing state above the first lasing threshold. We find that above the lasing threshold there is a whole continuum of exact plane-wave solutions. In order to pose the question of transverse instability and pattern formation, it is of great importance to ensure that the proper lasing state is investigated. We argue using a combination of amplitude expansions and numerical simulations that for negative detuning the flat amplitude state is selected above lasing threshold, whereas for positive detuning a single traveling wave with wave number k_0 is selected. Note in this latter case that even if the amplitude varies in the transverse direction, the intensity is still uniform. The linear stability of the lasing state is investigated for both signs of the detuning, and the predictions of the linear-stability analysis are verified by numerical simulations of the full system of equations.

The effect of adiabatic elimination of the polarization on the stability properties of the laser equations is also explored. We find the adiabatic elimination of the polarization alone leads to a system with very singular behavior lacking physical significance. Further adiabatic elimination of the inversion variable removes this singular behavior and produces a mathematically well-behaved system. However we note that the instability growth curves for this mathematically fully reduced system and the original problem are quite different. The inclusion of more terms in the expansion of the polarization does not remove any spurious singular behavior for positive detuning. An interesting alternative approach to adiabatic elimination in the Maxwell-Bloch equations based on the center-manifold theory, as outlined in Ref. [5], has recently been implemented [6]. Here, the adiabatic elimination of variables is analyzed in the case of no diffusion [6] for wide- and narrow-gain-section lasers. The theory, as outlined in Ref. [5] however, strictly only applies to cases where the center manifold is finite dimensional and could lead to spurious high-wave-number instabilities if formally applied in more general situations [7]. This spurious high-wave-number behavior appears in Fig. 3(b) of Ref. [6] for positive detuning. Doing the reduction in a manner that does not introduce high-wave-number instabilities is an important and so far unresolved problem.

BASIC EQUATIONS AND STABLE LASING SOLUTIONS

The semiclassical equations describing the dynamics of a homogeneously broadened, single-longitudinal-mode, unidirectional ring laser have been derived and studied by many authors [2–4,8,9], see also the review in Ref. [10]. Including diffraction and diffusion of the inversion, but assuming the mean-field limit to hold, the laser equations are

$$\frac{\partial E}{\partial t}+\mu E-ia\frac{\partial^2 E}{\partial x^2}=\beta_1 P \ , \tag{1}$$

$$\frac{\partial P}{\partial t}+\gamma_1(1+i\Delta)P=\beta_2 EN \ , \tag{2}$$

$$\frac{\partial N}{\partial t}+\gamma_2(N-N_0)-D\frac{\partial^2 N}{\partial x^2}=-\tfrac{1}{2}\beta_2(EP^*+E^*P) \ , \tag{3}$$

where E,P are the slowly varying electric-field and polarization envelopes, N is the inversion of the two-level system, μ is the cavity-decay constant, γ_1 is the polarization dephasing time, γ_2 is the inversion-decay time, β_1 and β_2 are coupling constants proportional to the dipole coupling between the lower and upper levels, N_0 is the pumping level, a is the diffraction, Δ is the detuning between the cavity and the atomic line, and D is the diffusion coefficient for the inversion.

The system (1)–(3) has two different equilibrium solutions depending on the value of the pumping parameter N_0. The first solution is $E=P=0$, $N=N_0$ and corresponds to the laser being below threshold. The second solution corresponds to lasing and is given by

$$\begin{bmatrix} E \\ P \end{bmatrix}=\begin{bmatrix} \bar{E} \\ \bar{P} \end{bmatrix}e^{i(k_0 x+\Omega t)}, \quad N=\bar{N}$$

where $\bar{E}$, $\bar{P}$, $\bar{N}$, and Ω are given by

$$\begin{aligned}
\bar{E}&=\left[\frac{\gamma_2\beta_1}{\mu\beta_2}(N_0-\bar{N})\right]^{1/2} \\
\bar{P}&=\frac{\mu+i(\Omega+ak_0^2)}{\beta_1}\bar{E} \ , \\
\bar{N}&=\frac{\mu\gamma_1}{\beta_1\beta_2}\left[1+\left[\frac{\gamma_1\Delta-ak_0^2}{\gamma_1+\mu}\right]^2\right] \ , \\
\Omega&=-\gamma_1\frac{\mu\Delta+ak_0^2}{\gamma_1+\mu} \ .
\end{aligned} \tag{4}$$

Note that the wave number k_0 is a free parameter. It is interesting and surprising that the full nonlinear system of equations (1), (2), and (3) actually have simple spatially dependent traveling-wave solutions. All these solutions will have homogeneous intensity, but they will have different amplitudes and frequencies depending on the value of the wave number k_0. For $k_0=0$ they reduce to the homogeneous solution studied in Ref. [3]. We are presently interested in finding the transition to states with nonhomogeneous intensity, or the so-called second-laser threshold. This transition will happen when the homogeneous intensity solution loses its stability to sideband perturbations. In order to do this correctly we must determine which of the solutions (4) the laser selects above the first-laser threshold. One finds this solution by linearizing the laser equations around the nonlasing solution and calculating which wave number k^c will have the highest growth rate at threshold. We will argue that this is the wave number the laser actually chooses, so when we study the second-laser threshold we set $k_0=k^c$ and investigate the stability of the corresponding traveling-wave solution.

Writing $P=p$, $E=e$, and $N=N_0+n$, where p,e,n are assumed to be small perturbations, we find by linearization of (1), (2), and (3)

$$e_t+\mu e-ia\frac{\partial^2 e}{\partial x^2}=\beta_1 p \ , \tag{5}$$

$$p_t+\gamma_1(1+i\Delta)p=\beta_2 eN_0 \ , \tag{6}$$

$$n_t+\gamma_2 n-D\frac{\partial^2 n}{\partial x^2}=0 \ . \tag{7}$$

Without loss of generality we may assume that the solution is of the form

$$\begin{bmatrix} e \\ p \\ n \end{bmatrix}=\begin{bmatrix} e_0 \\ p_0 \\ n_0 \end{bmatrix}e^{\lambda t+ikx} \ ,$$

where k is the perturbation wave number. The characteristic polynomial for λ is

$$(\lambda+\gamma_2+Dk^2)\{(\lambda+\mu+iak^2)[\lambda+\gamma_1(1+i\Delta)] -\beta_1\beta_2 N_0\}=0 \ .$$

One eigenvalue is $\lambda=-\gamma_2-Dk^2$. This eigenvalue does not contribute to instability for any parameter values since γ_2 and D are both positive. The two other roots are found to give instability when the pumping N_0 is above the threshold value N^c

$$N_0>N^c=\frac{\mu\gamma_1}{\beta_1\beta_2}\left[1+\left[\frac{\gamma_1\Delta-ak^2}{\gamma_1+\mu}\right]^2\right] \ . \tag{8}$$

We observe from Eqs. (4) that N^c is equal to the amplitude $\bar{N}$ for the lasing solution. The threshold for instability of the nonlasing solution coincides with the threshold for existence of the lasing solution as it should. The threshold condition (8) is the same as the one derived in Ref. [4]. It is now evident that the laser solution with the lowest threshold is $k_c=0$ when $\Delta<0$ and $k^c=\pm\sqrt{\gamma_1\Delta/a}$ when $\Delta>0$. This indicates that the laser above the first-laser threshold will select the solution (4) with $k_0=0$ when $\Delta<0$. For $\Delta>0$ we can only conclude that two wave numbers will grow initially. There are now several possible finite-amplitude states to choose from. One possibility is that the finite-amplitude state will be a standing wave, another possibility is that it will be a traveling wave, finally it is possible that neither of the above will happen. This problem is most easily resolved by direct numerical simulation of the system (1), (2), and (3). Figure 1 is a picture of the time evolution of the power spectrum (spatial Fourier transform) of the electric field above the first-laser threshold. This corresponds to the far-field output of the laser. The parameter values are $\mu=0.1$, $\beta_1=0.5$, $\beta_2=0.5$, $\delta=1$, $\gamma_1=10$, $\gamma_2=2$, $N_0=10$. The initial condition was a Gaussian perturbation on the nonlasing state. We observe that initially two wave numbers start growing, but eventually one of them wins out and the other vanishes. Figure 2 displays the last time frame from Fig. 1. The wave number selected

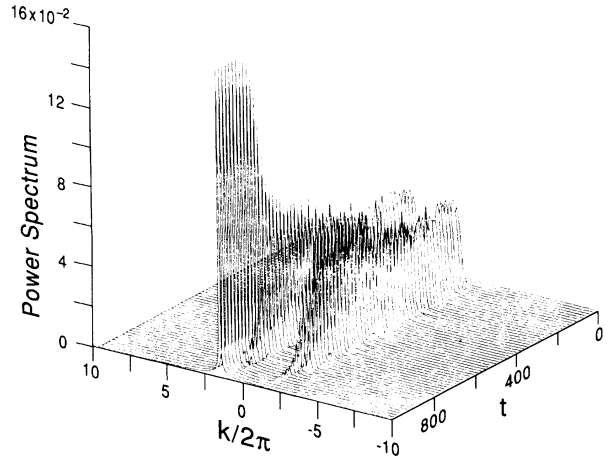

FIG. 1. Time evolution of the power spectrum of the electric field above the first-laser threshold but below the second-laser threshold. The parameter values are $\beta_1=0.5$, $\beta_2=0.5$, $\gamma_1=10$, $\gamma_2=2$, $\mu=0.1$, $a=0.1$, $N_0=10$.

is, in absolute value, exactly the one predicted by the formula for k_c with the given parameter values. This, taken together with the fact that (4) are exact traveling-wave solutions, leads us to conclude that (4) with $k_0=\pm\sqrt{\gamma_1\Delta/a}$ attracts nonlasing initial conditions in some region above the first-laser threshold. Physically, this result suggests that the laser will emit at a finite angle relative to the laser axis in wide-gain systems. In two transverse dimensions the output would be expected to grow as a ring whose angle subtended to the laser axis is a function of γ_1, Δ, and a. Using the linear-stability analysis from the next section we know that both left- and right-traveling waves are linearly stable in some region above the first-laser threshold so that whether the system chooses right- or left-going waves probably depends on the noise present in the system. In fact, in an extended region one could imagine that different regions might end up supporting traveling waves in different directions corresponding, for example, to front propagation. This single numerical simulation does not in any way prove that the standing wave is always unstable. For one space dimension there is, however, a more compelling argument based on the application of weakly nonlinear theory close to the first laser threshold. The basic idea of this method is to expand all field quantities to first order in the unstable modes of the linearized system at threshold. The dynamics of the amplitudes of this expansion are then chosen so as to keep corrections to the first order small in time and space. In this way one derives a, usually smaller, system of equations describing the evolution of the original system close to threshold. A good tutorial description of this method is given in Ref. [11]. A good feature of this method is that it tends to produce universal equations. For the case of positive detuning there are two unstable modes at the first-laser threshold, corresponding to left- and right-traveling waves, and so we need two amplitudes in order to apply the weakly nonlinear theory. The two amplitudes satisfy the following set of equations [12]:

$$\partial_t A_1=\frac{\beta_1\beta_2 N'}{\mu+\gamma_1}A_1-\frac{2a\gamma_1 k_c}{\mu+\gamma_1}\partial_x A_1+\frac{4\mu\gamma_1 a^2 k_c^2}{(\mu+\gamma_1)^3}\partial_{xx}A_1-i\frac{a\gamma_1}{\mu+\gamma_1}\partial_{xx}A_1-\frac{\mu\beta_2^2}{\gamma_2(\mu+\gamma_1)}[(1+s)A_1|A_2|^2+A_1|A_1|^2]$$

and

$$\partial_t A_2=\frac{\beta_1\beta_2 N'}{\mu+\gamma_1}A_2+\frac{2a\gamma_1 k_c}{\mu+\gamma_1}\partial_x A_2+\frac{4\mu\gamma_1 a^2 k_c^2}{(\mu+\gamma_1)^3}\partial_{xx}A_2-i\frac{a\gamma_1}{\mu+\gamma_1}\partial_{xx}A_2-\frac{\mu\beta_2^2}{\gamma_2(\mu+\gamma_1)}[(1+s)A_2|A_1|^2+A_2|A_2|^2]\,, \quad (9)$$

where $s=[1+(D/a)\gamma_1/\gamma_2]^{-1}$ and N' is the pumping above threshold. The linear parts of these equations are essentially the dispersion relation for the linearized system at threshold, expanded to second order close to the top of the two bands of unstable wave numbers. These are two coupled complex Ginsburg-Landau (CGL) equations and are typical for the type of equations that this method produces in systems close to threshold. The solution with $A_1=A_2$ corresponds to the standing-wave solution in the original system. In the Appendix we show that the solution with $A_1=A_2$ is always unstable for the coupled CGL equations (9). This supports our earlier claim that the laser will select the traveling-wave solution above threshold.

When investigating pattern-forming transverse insta-

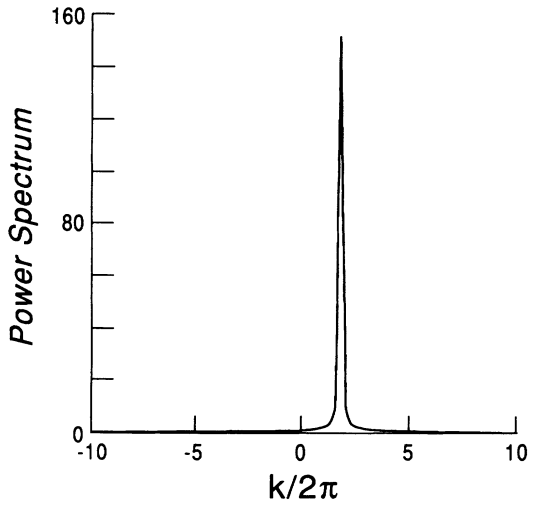

FIG. 2. The last time slice from Fig. 1. The parameter values are $\beta_1=0.5$, $\beta_2=0.5$, $\gamma_1=10$, $\gamma_2=2$, $\mu=0.1$, $a=0.1$, $N_0=10$.

bilities in this laser model it is very important to be aware of the fact that it is a traveling-wave solution that is selected by the laser at the first-laser threshold. The linear-stability analysis must be performed on this solution when $\Delta>0$ and not on the flat $k_0=0$ solution. A linear-stability analysis of the flat solution will predict an instability above the first-laser threshold that is not related to pattern formation but only to the fact that the traveling state is stable and attracting, at least locally. The presence of the nonzero wave number for $\Delta>0$, but not for $\Delta<0$, can be understood physically as a resonance phenomenon: The polarization has a natural oscillation at frequency $-\gamma_1\Delta$. A wave number k gives the electric field an oscillation component at frequency $-ak^2$. The inversion N is driven by (P^*E+PE^*). The frequency of this driving term will then be $\pm(\gamma_1\Delta-ak^2)$. If $\Delta<0$ the wave number that gives strongest coupling through the inversion will be $k=0$. On the other hand, if $\Delta>0$ the wave number that gives strongest coupling will be $k=\pm\sqrt{\gamma_1\Delta/a}$.

Since the far field of the laser output is essentially the Fourier transform of the near field, the physical implication of this result is that a controlled-beam steering may be achieved through, for example, piezoelectric tuning of the cavity. From a numerical point of view the existence of this traveling-wave instability can present a problem unless the field quantities are redefined such that the wave number k_0 is taken explicitly into account.

LINEAR STABILITY OF THE LASING SOLUTION IN THE UNREDUCED MODEL

We will investigate in this section the linear stability of the lasing solution with transverse wave number as derived in the last section. Using standard linear-stability methods we write

$$E=(\bar{E}+e)e^{i(k_0x+\Omega t)}, \tag{10}$$

$$P=(\bar{P}+p)e^{i(k_0x+\Omega t)}, \tag{11}$$

$$N=\bar{N}+n, \tag{12}$$

where e,p,n are assumed to be small perturbations. The linearized system for the perturbed quantities is

$$e_t+[\mu+i(\Omega+ak_0^2)]e=-2ak_0e_x+ia\frac{\partial^2 e}{\partial x^2}+\beta_1 p, \tag{13}$$

$$p_t+[\gamma_1+i(\Omega+\gamma_1\Delta)]p=\beta_2(\bar{N}e+\bar{E}n), \tag{14}$$

$$n_t+\gamma_2 n-D\frac{\partial^2 n}{\partial x^2}=-\beta_2\bar{E}\,\mathrm{Re}(p^*+\alpha^*e), \tag{15}$$

where $\alpha=\mu+i(\Omega+ak_0^2)]/\beta_1$. The stability of the lasing solution, or in other words, the position of the second-laser threshold, is found by looking for exponentially growing plane-wave-mode solutions for (13)–(15). Inserting such a trial solution gives a linear system of equations for the amplitudes with matrix A given by

$$\begin{bmatrix} \eta_1^r-2ak_0 & -\eta_1^i-ak^2 & -\beta_1 & 0 & 0 \\ \eta_1^i+ak^2 & \eta_1^r-2ak_0 & 0 & -\beta_1 & 0 \\ -\beta_2\bar{N} & 0 & \eta_2^r & -\eta_2^i & -\beta_2\bar{E} \\ 0 & -\beta_2\bar{N} & \eta_2^i & \eta_2^r & 0 \\ \beta_2\alpha^r\bar{E} & \beta_2\alpha^i\bar{E} & \beta_2\bar{E} & 0 & \gamma_2+Dk^2 \end{bmatrix}, \tag{16}$$

where $\eta_1^r,\eta_1^i,\eta_2^r,\eta_2^i$ are the real and imaginary parts of $\eta_1=\mu+i(ak_0^2+\Omega)$ and $\eta_2=\gamma_1+i(\Omega+\gamma_1\Delta)$. The wave number of the perturbing plane wave is k. The laser solution is unstable to the growth of the plane wave with wave number k if the matrix A has at least one eigenvalue with positive real part. Our point here is to compare the behavior of this stability problem with the corresponding one for the adiabatically reduced system. In Fig. 3 the first- and second-laser thresholds are graphed as a function of pumping and detuning. These curves were obtained for each value of pumping and detuning by finding the wave number k with highest growth rate and then looking for the zeros of this function. Figure 3 is computed with parameter values corresponding to the good-cavity limit. The relative disposition of the first- and second-threshold instability curves will be a sensitive function of the problem parameters. Here we indicate general trends in behavior. First, in the good-cavity limit under consideration here, the second-laser thresholds shift to lower pumping values as $\gamma_1\to\gamma_2$. Also note that for negative detuning in a certain range the system can go from stable to unstable and back to stable by increasing the pumping of the system. The actual shape of the growth curve for the perturbation is very different depending on the sign of the detuning. Figures 4 and 5 show the growth curve for positive and negative detuning, respectively, above the second-laser threshold. Observe the very different character of the two curves. For negative detuning we predict that a single group of closely spaced wave numbers will start growing, whereas for

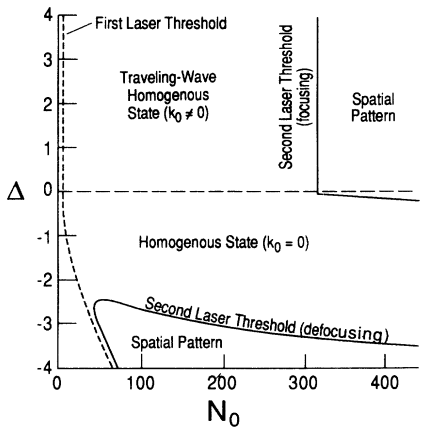

FIG. 3. The second-laser threshold in the plane of detuning Δ and pumping N_0. Parameter values $\beta_1=0.5$, $\beta_2=0.5$, $\gamma_1=10$, $\gamma_2=2$, $\mu=0.1$, $a=0.05$.

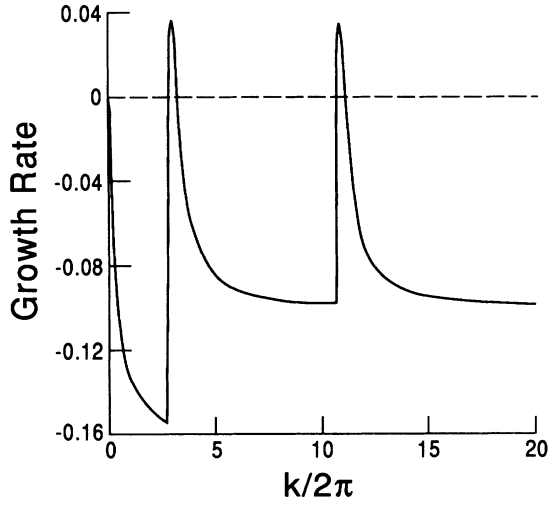

FIG. 4. The largest real part of any eigenvalue as a function of wave number k for the full problem. Parameter values are $\beta_1=0.5$, $\beta_2=0.5$, $\gamma_1=10$, $\gamma_2=2$, $\mu=0.1$, $a=0.05$, $\Delta=3$, $N_0=700$.

positive detuning two separate groups of wave numbers will start growing at the same time. When the detuning goes to zero from the positive side the two groups of wave numbers come together to form a single group. Remembering that for positive detuning the laser solution we are perturbing around has its own nonzero wave number; we recognize the much more complicated dynamics when $\Delta>0$. The experimental detection of these complicated solutions may be difficult because of the extremely high values of N_0. Interesting pattern formation at pump values within experimental feasibility is predicted in the defocussing case $\Delta<0$. Figures 6 and 7 show the time evolution of the corresponding power spectra of

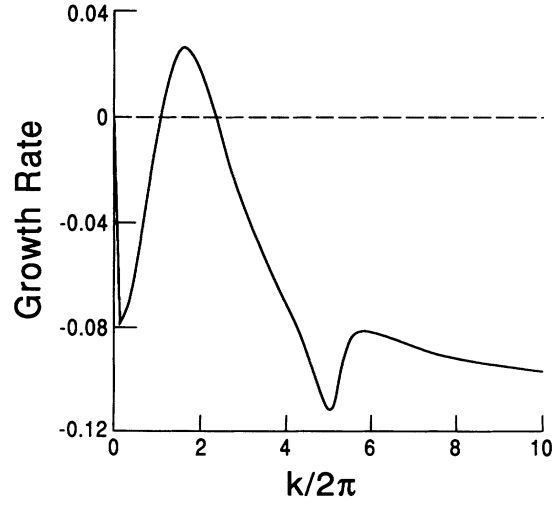

FIG. 5. The largest real part of any eigenvalue as a function of wave number k for the full problem. Parameter values are $\beta_1=0.5$, $\beta_2=0.5$, $\gamma_1=10$, $\gamma_2=2$, $\mu=0.1$, $a=0.05$, $\Delta=-4$, $N_0=300$.

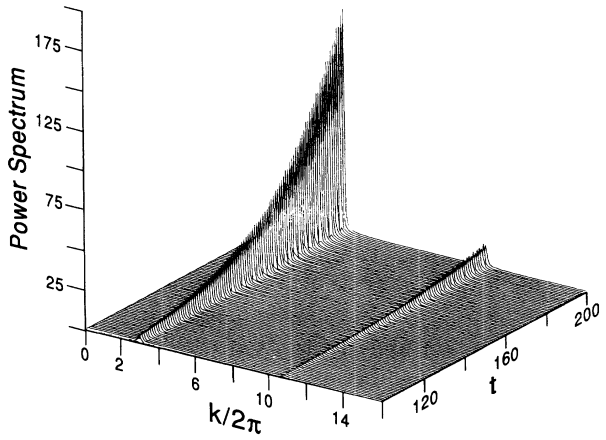

FIG. 6. The time evolution of the power spectrum of the electric field as a function of time for positive detuning for the full system. The parameter values are the same as in Fig. 4.

the electric field for the same parameter values as in Fig. 4 and Fig. 5. The predicted instability behavior is clearly confirmed by the numerical simulations.

ADIABATIC ELIMINATION AND STABILITY OF THE REDUCED MODEL

In this section we will use standard adiabatic elimination to derive a reduced system of equations involving E and N only. Our main objective is to show, by using linear-stability analysis and supporting it with numerical simulations, that the reduced system is very badly behaved. The laser model is

$$\frac{\partial \mathcal{E}}{\partial t}+\mu\mathcal{E}-ia\frac{\partial^2\mathcal{E}}{\partial x^2}=\beta_1\mathcal{P}\ , \tag{17}$$

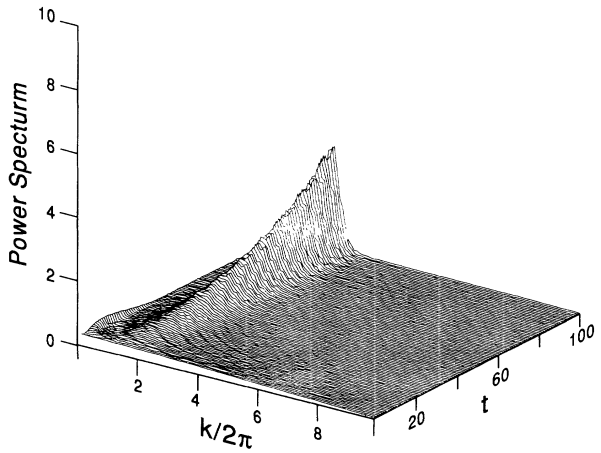

FIG. 7. The time evolution of the power spectrum of the electric field as a function of time for negative detuning for the full system. The parameter values are the same as in Fig. 5.

$$\frac{\partial \mathcal{P}}{\partial t}+\gamma_1(1+i\Delta)\mathcal{P}=\beta_2\mathcal{E}N \ , \tag{18}$$

$$\frac{\partial N}{\partial t}+\gamma_2(N-N_0)-D\frac{\partial^2 N}{\partial x^2}=-\tfrac{1}{2}\beta_2(\mathcal{E}\mathcal{P}^*+\mathcal{E}^*\mathcal{P}) \ . \tag{19}$$

The equation for $\mathcal{P}$ can be solved formally to yield

$$\mathcal{P}=\beta_2\int_0^\infty e^{-\gamma_1(1+i\Delta)s}\mathcal{E}N(t-s)ds \ . \tag{20}$$

The assumption underlying adiabatic elimination is that the polarization dephasing time γ_1 is much faster than all other time scales in the problem. Since diffraction is included in the electric-field equation we also must assume that there is little energy in modes with wave numbers that correspond to frequencies that are of the order of γ_1 or bigger. With this in mind we can solve the integral in (20) using standard asymptotic techniques [13]. The main feature is that we expand $\mathcal{E}(t-s)$ in a Taylor series around $s=0$ and integrate this series term by term. The resulting expression for $\mathcal{P}$ is

$$\mathcal{P}\approx\frac{\beta_2}{[\gamma_1(1+i\Delta)]}\mathcal{E}N-\frac{\beta_2}{[\gamma_1(1+i\Delta)]^2}\partial_t(\mathcal{E}N) \ . \tag{21}$$

As a first approximation we will keep only terms of first order in $1/\gamma_1$ in (21). The time derivative in (21) is evaluated using the linear part of the field equations (1), (2), assuming that the nonlinear coupling is small. The reduced system of equations can, by rescaling, be put into the form

$$\begin{aligned}&\frac{\partial E}{\partial t}+\mu E-\tfrac{1}{2}\beta(1-i\Delta)EN-ia\frac{\partial^2 E}{\partial x^2}=0 \ ,\\ &\frac{\partial N}{\partial t}+\gamma_2(N-N_0)-D\frac{\partial^2 N}{\partial x^2}+\beta|E|^2N=0 \ ,\end{aligned} \tag{22}$$

where β is a new coupling constant. The reduced system (22), like the full system, has two different stationary solutions corresponding to a nonlasing and a lasing state. The lasing solution is

$$E=\bar{E}e^{i(k_0x+\Omega t)}, \quad N=\bar{N} \ ,$$

where

$$\bar{E}=\left[\frac{\gamma_2}{2\mu}(N_0-\bar{N})\right]^{1/2} \ , \tag{23}$$

$$\bar{N}=\frac{2\mu}{\beta} \ , \tag{24}$$

$$\Omega=-\mu\Delta-ak_0^2 \ . \tag{25}$$

In this case the first laser threshold does not favor any wave number. We will investigate the stability of the homogeneous state $k_0=0$ since numerical simulations seem to favor this state in the regime where the laser solution is stable. Our main conclusion about the singular behavior of the reduced system could be derived by investigating the instability of any of the solutions corresponding to $k_0\neq 0$.

Linearize the reduced system by writing

$$E=(\bar{E}+e)e^{i(k_0x+\Omega t)}, \quad N=\bar{N}+n$$

where as usual e and n are small perturbations. Keeping only linear terms from (22), we find

$$e_t=\tfrac{1}{2}\beta(1-i\Delta)\bar{E}n+ia\frac{\partial^2 e}{\partial x^2} \ , \tag{26}$$

$$n_t=-(\gamma_2+\beta\bar{E}^2)n-\beta\bar{E}\,\bar{N}(e+e^*)+D\frac{\partial^2 n}{\partial x^2} \ . \tag{27}$$

The growth rate of plane-wave solutions with wave number k is determined by the real part of the solutions of the following characteristic polynomial:

$$(s+p)(s^2+1)-q(\Delta-s)=0 \ , \tag{28}$$

where

$$\begin{aligned}p&=\frac{1}{ak^2}(\gamma_2+\beta\bar{E}^2+Dk^2) \ ,\\ q&=\frac{\beta^2\bar{E}^2\bar{N}}{(ak^2)^2} \ ,\\ s&=\frac{\lambda}{ak^2} \ .\end{aligned} \tag{29}$$

Written in this form it is straightforward to find that the characteristic polynomial has solutions with positive real part only if

$$p+\Delta<0, \quad p-q\Delta<0 \ .$$

Using the expressions for p and q we find that the conditions for a plane-wave perturbation with wave number k to grow are

$$N_0>\frac{2\mu\Delta+aDk^4}{\gamma_2(\beta\Delta-ak^2/\bar{N})}, \quad \Delta>0 \ , \tag{30}$$

$$\bar{N}<N_0<\bar{N}\left[\frac{ak^2}{\gamma_2}\left[|\Delta|-\frac{D}{a}\right]\right], \quad \Delta<0 \ . \tag{31}$$

Observe that the second-laser threshold as a function of pumping and detuning is just a straight line vertical to the pump axis. This is in sharp contrast to the complicated shape displayed by the second-laser threshold for the full system in Fig. 3.

We will for simplicity first consider the case without inversion diffusion, $D=0$. In this case condition (30) implies that all wave numbers below a certain maximum wave number are unstable

$$k^2<\frac{2\Delta\mu}{a}\left[1-\frac{\bar{N}}{N_0}\right] \ . \tag{32}$$

This is a long-wavelength instability similar to the Benjamin-Feir instability [14] for the nonlinear Schrödinger equation. In fact if the inversion is also adiabatically eliminated and the weak-field limit assumed, then this instability becomes exactly the Benjamin-Feir instability. Note that this behavior is very different from the instability for the full system with $\Delta>0$.

The second condition (31) with $D=0$ shows that all wave numbers above a certain minimum wave number are unstable

$$k^2 > \frac{\gamma_2}{a|\Delta|} . \tag{33}$$

This is a short-wavelength instability that clearly is not physical and must be a result of the adiabatic elimination of the polarization. Figures 8 and 9 show the growth curve for positive and negative detuning, respectively. The infinite tail of the positive-growth rate is evident in Fig. 9. Note that apart from the infinite tail, which induces unphysical short-wave instabilities, the growth curve for the reduced system when $\Delta<0$ is qualitatively similar to the growth curve for the full system in Fig. 5. Also observe that the growth rate for positive detuning ($\Delta>0$) seems to be approaching zero from below. Center-manifold methods appear to remove these spurious instabilities for negative detuning [6]. In order to investigate the high-wave-number behavior of the growth curve more closely, we have used perturbation methods to derive an asymptotic expression for large k

$$\lambda \approx -\frac{\beta^2 \bar{E}^2 \bar{N}^2}{2} \frac{D+a\Delta}{D^2+ak^2} . \tag{34}$$

From (34) it is clear that the growth rate actually goes to zero from below for large k and positive detuning. This behavior has very serious consequences. If the system is simulated numerically with positive detuning above the second laser threshold, the low-wave-number instability will excite the highest wave number supported on the computational grid, and the simulation will fail due to loss of accuracy. The presence of any amount of inversion diffusion will not remove this singular behavior when the detuning is positive as is evident from (34). From (31) and (34) it is, however, clear that when the detuning is negative and $D>a|\Delta|$, the instability is in fact gone. It seems paradoxical but is true that an inaccurate numerical scheme for the reduced equations behaves more reasonably than an accurate scheme, because the former will contain numerically generated diffusion that will tend to damp out high wave numbers. The predictions of the linear-stability analysis are clearly confirmed by Figs. 10 and 11, which show the time evolution of the power spectrum when the instability growth curve is given by Figs. 8 and 9, respectively. Note the similarity to a typical numerical instability.

We have seen that in general the instability growth curve for the full and reduced systems are very different. There are, however, also similarities worth noting. In the defocusing case $\Delta<0$ the growth curves for the full and

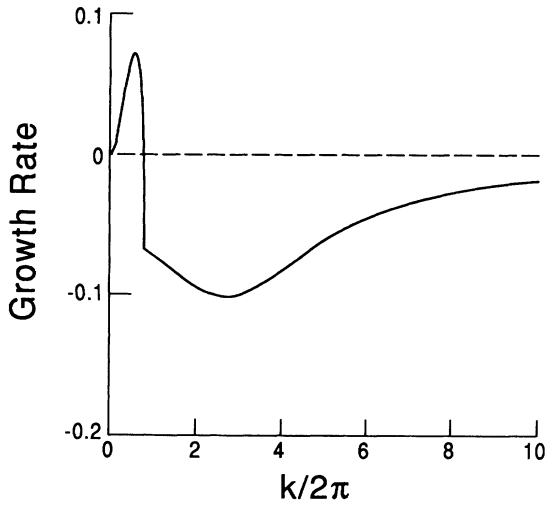

FIG. 8. The largest real part of any eigenvalue as a function of wave number k for the reduced problem for the case of positive detuning. Parameter values are $\beta=0.1$, $\gamma_2=2$, $\mu=0.1$, $a=0.01$, $\Delta=2$, $N_0=5$.

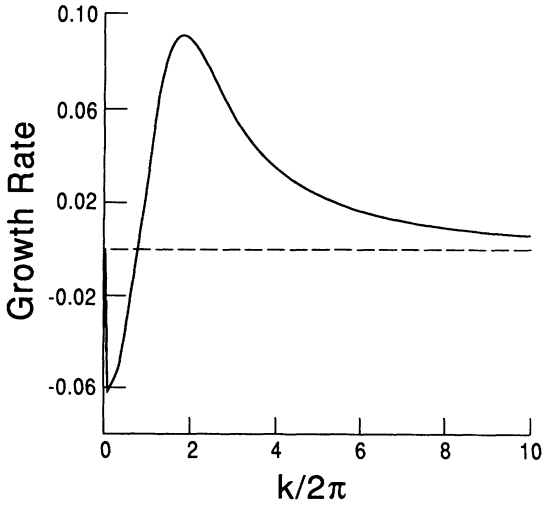

FIG. 9. The largest real part of any eigenvalue as a function of wave number k for the reduced problem for the case of negative detuning. Parameter values are $\beta=0.5$, $\gamma=2\mu=0.1$, $a=0.05$, $\Delta=-4$, $N_0=1$.

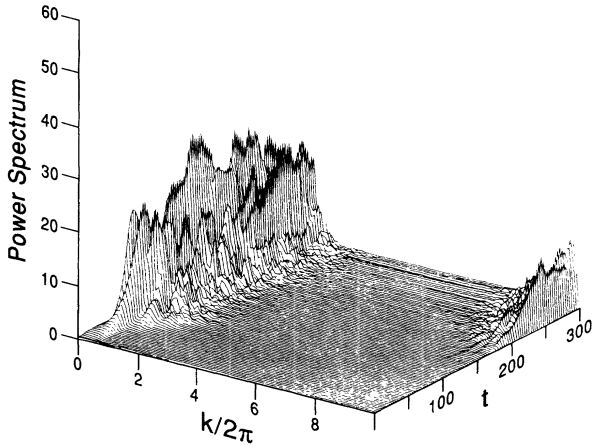

FIG. 10. The time evolution of the power spectrum of the electric field as a function of time for positive detuning for the reduced system. The parameter values are the same as in Fig. 8.

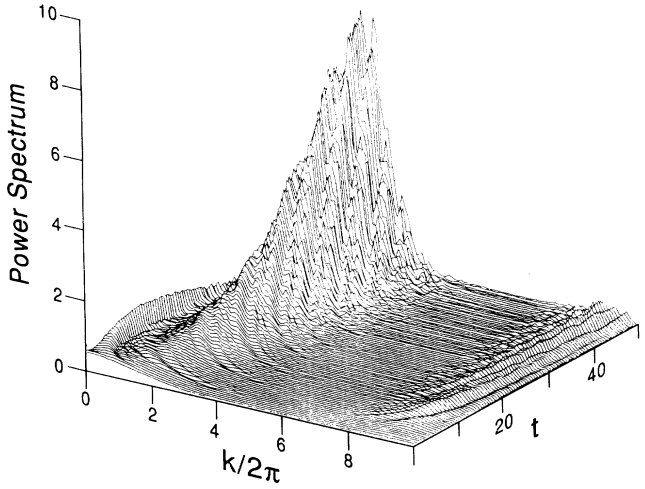

FIG. 11. The time evolution of the power spectrum of the electric field as a function of time for negative detuning for the reduced system. The parameter values are the same as in Fig. 9.

reduced systems are actually very similar in the low-wave-number regime. The main difference lies in the behavior of the tail at high spatial wave numbers. We have also investigated the fully reduced system obtained by also eliminating the inversion adiabatically, and for this system there is no singular behavior for either sign of the detuning. The growth curves for the full system and fully reduced system are, however, very different. In conclusion, the standard adiabatic elimination scheme breaks down for either sign of the detuning. Center-manifold methods [6] remove high-wave-number instabilities for negative detuning but fail for positive detuning.

DISCUSSION

From the results presented in the last two sections it is evident that direct adiabatic elimination does not work when there is diffraction present, even if the polarization dephasing time is much larger than the inversion- and cavity-decay times. The reason for the failure we believe is the slaving of the polarization to the motion of the electric field. This means that P and E will always vary on the same time scale, and P^*E will be slowly varying. Since the material equation is driven by a time average of P^*E, it will always have a finite driving and the self-consistent field-material loop is closed. On the other hand, if P is not slaved to E, then for high wave numbers P^*E will oscillate rapidly, the driving term in the inversion equation will average to zero, and the loop is broken. It could be argued that the problem may be fixed by retaining one or more terms in the adiabatic expansion for the polarization (21). We have investigated this, and we found that including one more term in the expansion did produce a system of equations that differs from the first-level equations (22) by the inclusion of several additional terms, the most important being a diffusion term in the equation for E. The sign of the diffusion coefficient is determined by the sign of Δ. When Δ is negative, the diffusion coefficient is positive, and the equation is well behaved. However when the detuning is positive, the diffusion coefficient is negative, and the diffusion terms acts like a reverse heat equation, and the system is totally singular. We believe that adiabatic elimination in the form presented here will never work at any level of truncation of the expansion (21) when $\Delta > 0$.

The present discussion has been presented for the case of one transverse dimension, but we are convinced that our conclusion also holds for two transverse dimensions and without the mean-field limit. The linear-stability analysis predicts the same type of asymptotic behavior for the growth curve for these cases. Pattern formation in two dimensions is currently under investigation.

CONCLUSION

We have pointed out that the equations for a homogeneously broadened, single-longitudinal-mode ring laser will start lasing in a traveling-wave state when $\Delta > 0$. This state would be observable in the far-field output of the laser as an off-axis emission. The wave number selected by this traveling-wave state can violate the assumptions underlying the derivation of the model equations. We have investigated the method of adiabatic elimination in the presence of diffraction and found that it fails to produce a well-behaved system of equations when it is applied to the equations for a homogeneously broadened ring laser. By including diffusion explicitly in the inversion equation, we have also established that the artificial instability introduced by adiabatic elimination cannot be removed. Center-manifold methods appear to remove successfully artificial instabilities in the defocusing case, but the positive-detuning case remains unresolved [6]. This result is particularly relevant when modeling semiconductor lasers with wide-gain sections as in multistripe or broad-area lasers.

ACKNOWLEDGMENTS

The authors wish to thank the Arizona Center for Mathematical Sciences (ACMS) for support. ACMS is sponsored by AFOSR Contract No. F49620-86-C0130 with the University Research Initiative Program at the University of Arizona. P.K.J. would like to thank the Norwegian Research Council for Sciences and Humanities (NAVF) for their generous support.

APPENDIX

In this section we will investigate the linear stability of the standing-wave solution for a set of coupled CGL equations of the form

$$\partial_t A_1 = \mu A_1 - \beta \partial_x A_1 + (\gamma - i\rho)\partial_{xx} A_1 - \eta[(1+s)A_1|A_2|^2 + A_1|A_1|^2], \quad \text{(A1)}$$

$$\partial_t A_2=\mu A_2+\beta\partial_x A_2+(\gamma-i\rho)\partial_{xx} A_2 -\eta[(1+s)A_2|A_1|^2+A_2|A_2|^2]\,, \tag{A2}$$

where $\mu,\beta,\gamma,\rho,\eta,s$ are real parameters. Standing-wave solutions are of the form

$$A_1=A_1^0 e^{i\delta_1 t},\quad A_2=A_2^0 e^{i\delta_2 t}\,. \tag{A3}$$

By substituting (A3) into (A1) and (A2) we find that $\delta_1=\delta_2=0$ and

$$\begin{aligned} 0&=\mu-\eta[(1+s)|A_2^0|^2+|A_1^0|^2]\,,\\ 0&=\mu-\eta[(1+s)|A_1^0|^2+|A_2^0|^2]\,. \end{aligned} \tag{A4}$$

We can now without loss of generality assume that A_1^0, A_2^0 both are real. The system (38) gives upon solution the standing-wave solution

$$A_1^0=A_2^0=\left[\frac{\mu}{\eta(s+2)}\right]^{1/2}. \tag{A5}$$

The linear stability of the standing-wave solution is investigated by perturbing the standing wave a small amount $A_1=A_1^0+a_1$, $A_2=A_2^0+a_2$ and deriving a linear system for the perturbations a_1,a_2. We find after linearization the following system for a_1,a_2:

$$\begin{aligned} \partial_t a_1&=\mu a_1-\beta\partial_x a_1+(\gamma-i\rho)\partial_{xx} a_1\\ &\quad-\eta\{[(1+s)A_1^0A_2^0(a_2+a_2^*)+(A_2^0)^2a_1]\\ &\quad+(A_1^0)^2a_1+(A_1^0)^2(a_1+a_1^*)\}\,,\\ \partial_t a_2&=\mu a_2+\beta\partial x a_2+(\gamma-i\rho)\partial_{xx} a_2\\ &\quad-\eta\{[(1+s)A_1^0A_2^0(a_1+a_1^*)+(A_1^0)^2a_2]\\ &\quad+(A_2^0)^2a_2+(A_2^0)^2(a_2+a_2^*)\}\,. \end{aligned} \tag{A6}$$

Take the Fourier transform of (41) and introduce new dependent variables $X=a_1+a_1^*$, $Y=a_2+a_2^*$, $U=a_1-a_1^*$, $V=a_2-a_2^*$. The matrix A of the resulting linear system of ordinary differential equations is

$$\begin{bmatrix} i\beta k-\gamma k^2-2\eta(A_1^0)^2 & -2\eta(1+s)A_1^0A_2^0 & i\rho k^2 & 0\\ -2\eta(1+s)A_1^0A_2^0 & i\beta k-\gamma k^2-2\eta(A_2^0)^2 & 0 & i\rho k^2\\ i\rho k^2 & 0 & i\beta k-\gamma k^2 & 0\\ 0 & i\gamma k^2 & 0 & -i\beta k-\gamma k^2 \end{bmatrix},$$

where k is the wave number of the perturbation. The standing wave is unstable to a perturbation with wave number k if the matrix A has any eigenvalues with positive real part. Consider the special case $k=0$. The characteristic polynomial for A when $k=0$ is

$$\lambda^2+2\eta[(A_1^0)^2+(A_2^0)^2]\lambda-4\eta^2 s(s+1)(A_1^0)^2(A_2^0)^2=0\,. \tag{A7}$$

This polynomial will clearly have two real roots, and one of them will always be positive. This proves that the standing wave is unstable to flat perturbations. By continuity it will in fact be unstable to perturbation with wave numbers in some band around $k=0$.

[1] L. A. Lugiato, G. L. Oppo, J. R. Tredicce, L. M. Narducci, and M. A. Pernigo, J. Opt. Soc. Am. B 7, 1019 (1990).

[2] L. M. Narducci, J. R. Tredicce, L. A. Lugiato, N. B. Abraham, and D. K. Bandy, Phys. Rev. A **33**, 1842 (1986).

[3] L. A. Lugiato, C. Oldano, and L. M. Narducci, J. Opt. Soc. Am. B **5**, 879 (1988).

[4] P. Coullet, L. Gil, and F. Rocca, Opt. Commun. **73**, 403 (1989).

[5] J. Carr, *Applications of Center Manifold Theory* (Springer, New York, 1981).

[6] Gian-Luca Oppo, Giampaolo D'Alessandro, and William L. Firth, Phys. Rev. A **44**, 4712 (1991).

[7] G. L. Oppo (private communication).

[8] L. A. Lugiato, L. M. Narducci, and M. F. Squicciarini, Phys. Rev. A **7**, 3101 (1986).

[9] H. Risken and K. Nummedal, J. Appl. Phys. **39**, 4662 (1968).

[10] N. B. Abraham, D. Dangoisse, Pierre Glorieux, and P. Mandel, JOSA B **2**, 23 (1985).

[11] *The Dynamics and Analysis of Patterns,* edited by D. Stein (Addison-Wesley, Reading, MA, 1989), pp. 1–67.

[12] P. K. Jakobsen, Ph.D. thesis, University of Arizona, 1990.

[13] C. M. Bender and S. A. Orszag, *Advanced Mathematical Methods for Scientists and Engineers* (McGraw-Hill, New York, 1978).

[14] T. B. Benjamin and J. F. Feir, J. Fluid Mech. **27**, 417 (1967).

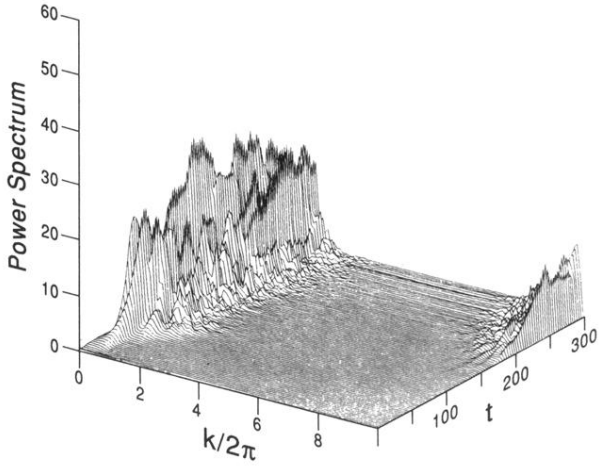

FIG. 10. The time evolution of the power spectrum of the electric field as a function of time for positive detuning for the reduced system. The parameter values are the same as in Fig. 8.

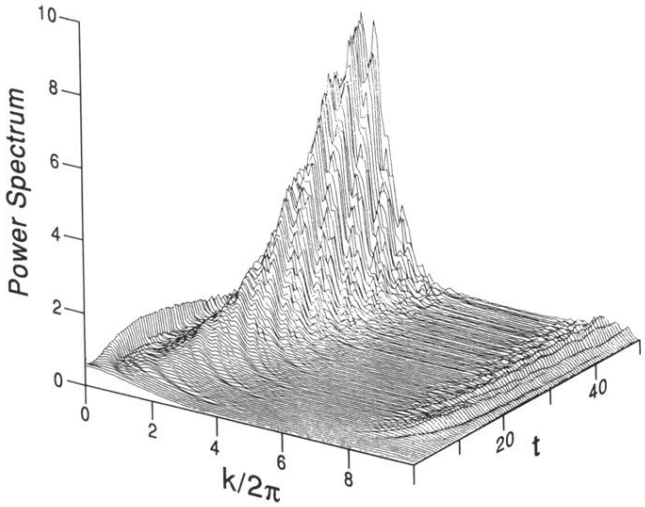

FIG. 11. The time evolution of the power spectrum of the electric field as a function of time for negative detuning for the reduced system. The parameter values are the same as in Fig. 9.

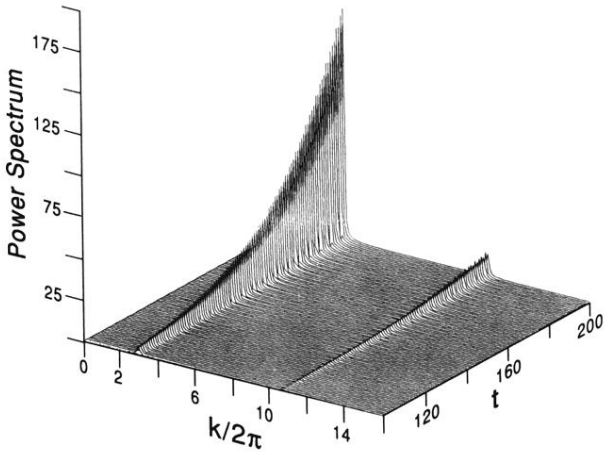

FIG. 6. The time evolution of the power spectrum of the electric field as a function of time for positive detuning for the full system. The parameter values are the same as in Fig. 4.

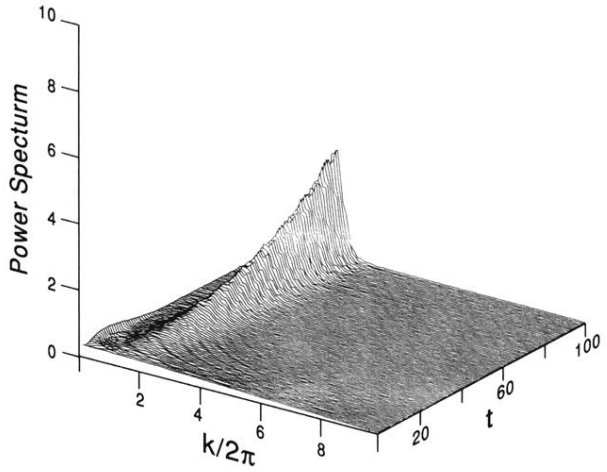

FIG. 7. The time evolution of the power spectrum of the electric field as a function of time for negative detuning for the full system. The parameter values are the same as in Fig. 5.